

Update on strong and radiative decays of the D_{s0}^* (2317) and D_{s1} (2460) and their bottom cousins

Hai-Long Fu^{a,1,2}, Harald W. Griebhammer^{b,3}, Feng-Kun Guo^{c,1,2}, Christoph Hanhart^{d,4},
Ulf-G. Meißner^{e,5,4,6}

¹ CAS Key Laboratory of Theoretical Physics, Institute of Theoretical Physics, Chinese Academy of Sciences, Beijing, 100190, China

² School of Physical Sciences, University of Chinese Academy of Sciences, Beijing, 100049, China

³ Institute for Nuclear Studies, Department of Physics, The George Washington University, Washington DC 20052, USA

⁴ Institute for Advanced Simulation, Institut für Kernphysik and Jülich Center for Hadron Physics, Forschungszentrum Jülich, D-52425 Jülich, Germany

⁵ Helmholtz-Institut für Strahlen- und Kernphysik and Bethe Center for Theoretical Physics, Universität Bonn, D-53115 Bonn, Germany

⁶ Tbilisi State University, 0186 Tbilisi, Georgia

Abstract The isospin breaking and radiative decay widths of the positive-parity charm-strange mesons, D_{s0}^* and D_{s1} , and their predicted bottom-strange counterparts, B_{s0}^* and B_{s1} , as hadronic molecules are revisited. This is necessary, since the B_{s0}^* and B_{s1} masses used in Eur. Phys. J. A **50** (2014) 149 [1] were too small, in conflict with the heavy quark flavour symmetry. Furthermore, not all isospin breaking contributions were considered. We here present a method to restore heavy quark flavour symmetry, correcting the masses of B_{s0}^* and B_{s1} , and include the complete isospin breaking contributions up to next-to-leading order. With this we provide updated hadronic decay widths for all of D_{s0}^* , D_{s1} , B_{s0}^* and B_{s1} . Results for the partial widths of the radiative decays of D_{s0}^* (2317) and D_{s1} (2460) are also renewed in light of the much more precisely measured D^{*+} width. We find that $B_s\pi^0$ and $B_s\gamma$ are the preferred channels for searching for B_{s0}^* and B_{s1} , respectively.

The lightest positive-parity charm mesons D_{s0}^* [2] and D_{s1} [3] are among the first observed heavy-flavour mesons with properties beyond quark model expectations. They are prominent candidates of hadronic molecules [4], with the dominant components residing in the isoscalar DK and D^*K channels, respectively. In particular, within the hadronic molecular picture, the approximate equality of the mass differences $M_{D^*} - M_D$ and $M_{D_{s1}} - M_{D_{s0}^*}$ is a natural consequence of heavy quark spin symmetry. Yet, this might also be explained in the chiral doublet model of Refs. [5, 6]. However, the partial decay widths of these states play a unique role in discriminating various models. In particular, the isospin breaking hadronic decays $D_{s0}^* \rightarrow D_s\pi^0$ and $D_{s1} \rightarrow D_s^*\pi^0$ are

expected to be much larger in the molecular approach than in other models, since in addition to the more conventional π^0 - η mixing mechanism, also the mass differences of charged and neutral constituents contribute via loops. Moreover, these contributions are large only for molecular states and enhanced by the nearby threshold cusps, a mechanism well known from the a_0 - f_0 mixing [7, 8].

Heavy quark flavour symmetry (HQFS) allows one to estimate the masses of the bottom partners of the D_{s0}^* and D_{s1} , independent of the model assumptions for their internal structure. One finds

$$M_{B_{s0}^*} = \bar{M}_c + \Delta_{b-c} + (M_{D_{s0}^*} - \bar{M}_c) \frac{m_c}{m_b} \simeq 5.71 \text{ GeV},$$
$$M_{B_{s1}} = \bar{M}_c + \Delta_{b-c} + (M_{D_{s1}} - \bar{M}_c) \frac{m_c}{m_b} \simeq 5.76 \text{ GeV}, \quad (1)$$

where $\bar{M}_c = (M_{D_{s0}^*} + 3M_{D_{s1}})/4 = 2.42 \text{ GeV}$ is the spin-averaged mass of the charmed mesons, Δ_{b-c} is the difference between the bottom and charm quark mass scales, which may be estimated by $\bar{M}_{B_s} - \bar{M}_{D_s} \simeq 3.33 \text{ GeV}$, with $\bar{M}_{B_s} = 5.40 \text{ GeV}$ and $\bar{M}_{D_s} = 2.08 \text{ GeV}$ the spin-averaged masses of the ground state pseudoscalar and vector $Q\bar{s}$ mesons. More precise results with controlled uncertainties in the hadronic molecular model can be found in Refs. [9, 10] and are consistent with these simple predictions; see also Refs. [11, 12]. The predictions of Ref. [13] for these masses are 5761 MeV and 5807 MeV, respectively, about 50 MeV higher. On the other hand, the lattice results in Ref. [14] are $M_{B_{s0}^*}^{\text{lat}} = (5711 \pm 13 \pm 19) \text{ MeV}$ and $M_{B_{s1}}^{\text{lat}} = (5750 \pm 17 \pm 19) \text{ MeV}$, also in nice agreement with the HQFS predictions (1).

So far, neither of these two bottom-strange mesons has been observed, but they are currently searched for at the LHCb experiment. It is therefore important and timely to have reliable predictions of both radiative and isospin breaking hadronic decay widths of these mesons. The predictions in the hadronic molecular model have been made in Refs. [1]

^afuhailong@itp.ac.cn

^bhgrie@gwu.edu

^cfkguo@itp.ac.cn

^dc.hanhart@fz-juelich.de

^emeissner@hiskp.uni-bonn.de

(see also Refs. [15–22] for predictions of some of the states and Refs. [23, 24] for calculations in chiral perturbation theory up to one-loop order). However, the B_{s0}^* and B_{s1} masses used there, (5625 ± 45) MeV and (5671 ± 45) MeV, respectively, are too low to be consistent with the HQFS expectations derived from Eq. (1). Consequently, the partial decay widths computed therein need to be corrected.

The low masses for the bottom strange scalar states in Ref. [1] can be traced to a heavy-quark mass independent subtraction constant used to regularize the two-point scalar loop integral. However, a proper matching procedure unavoidably requires a heavy-quark mass dependence of this quantity. To see this observe that the two-point loop integral, which includes the right-hand cut, is ultraviolet divergent and can be regularized in different ways. One option is to use dimensional regularization with a subtraction constant $a(\mu)$, where the regularization scale μ may be taken to be 1 GeV; variations of this value can be absorbed into the related variation of $a(\mu)$. Alternatively, the ultraviolet divergence can be regularized by a hard cutoff, q_{\max} , on the magnitude of the loop three-momentum. We denote the resulting two-point scalar loop functions by $G_{\text{sub}}(s, a(\mu))$ and $G_{\text{CO}}(s, q_{\max})$, respectively, with s the c.m. energy squared.

In the previous analysis [25], where the low-energy constants were determined, the method with a subtraction constant was used. However, the dependence of the subtraction constant on the heavy quark mass, m_Q , is not clear a priori. In order to take this into account, it was proposed in Ref. [11] to match G_{sub} and G_{CO} at the relevant charmed meson threshold to determine q_{\max} from a given $a(\mu)$, and then use the same q_{\max} in the bottom sector at a relevant bottom threshold to determine the value of $a(\mu)$ there. Since the value of $q_{\max} \sim 0.8$ GeV is much smaller than the charmed meson mass, HQFS should be well preserved in this way.¹

To be specific, the expressions for the loop functions $G_{\text{sub}}(M_{\text{thr}}^2, a(\mu))$ and $G_{\text{CO}}(M_{\text{thr}}^2, q_{\max})$ at the HK threshold, $M_{\text{thr}} = M_H + M_K$, are given by

$$\begin{aligned} G_{\text{sub}}(M_{\text{thr}}^2, a(\mu)) &= \frac{1}{16\pi^2} \left[a(\mu) + \frac{1}{M_{\text{thr}}} \sum_{i=H,K} M_i \log \frac{M_i^2}{\mu^2} \right], \\ G_{\text{CO}}(M_{\text{thr}}^2, q_{\max}) &= \frac{1}{16\pi^2 M_{\text{thr}}} \sum_{i=H,K} M_i \log \frac{M_i^2}{\left(\sqrt{M_i^2 + q_{\max}^2} + q_{\max} \right)^2}. \end{aligned} \quad (2)$$

The matching requires

$$G_{\text{sub}}(M_{\text{thr}}^2, a(\mu)) = G_{\text{CO}}(M_{\text{thr}}^2, q_{\max}), \quad (3)$$

¹The procedure was also described in the previous study [1]; however, it was unfortunately not implemented in the code, and thus the masses of the B_{s0}^* and B_{s1} obtained and used therein were too small.

Table 1: Masses of the lowest positive-parity heavy-strange mesons [9, 10] and their effective couplings, g_1 and g_2 , respectively, to the isoscalar $D^{(*)}K$ and $D_s^{(*)}\eta$ ($\bar{B}^{(*)}K$ and $\bar{B}_s^{(*)}\eta$) channels predicted using the parameters in Ref. [25] after the proper scaling of the subtraction constant. The mass of the $D_{s0}^*(2317)$ is fixed in obtaining the parameters. The masses and couplings are given in units of MeV and GeV, respectively.

Meson	Mass	g_1	g_2
D_{s0}^*	2318 (fixed)	9.4 ± 0.3	7.4 ± 0.1
D_{s1}	2458_{-17}^{+15}	$10.1_{-0.9}^{+0.8}$	7.9 ± 0.3
B_{s0}^*	5722 ± 14	$22.9_{-1.5}^{+1.3}$	$18.8_{-0.5}^{+0.4}$
B_{s1}	5774 ± 13	$22.5_{-1.5}^{+1.3}$	18.7 ± 0.5

which leads to the heavy-meson-mass (M_H) dependence of $a(\mu)$ as

$$a(\mu) = \frac{1}{M_{\text{thr}}} \sum_{i=H,K} M_i \log \frac{\mu^2}{\left(\sqrt{M_i^2 + q_{\max}^2} + q_{\max} \right)^2}. \quad (4)$$

For the mass dependence of $a(\mu)$, see also Ref. [26].

In the charm sector we obtain for $M_{\text{thr}} = M_{D_s} + M_K$ and $a_D(1 \text{ GeV}) = -1.87_{-0.04}^{+0.05}$ [25] the three-momentum cutoff

$$q_{\max} = 745_{-37}^{+35} \text{ MeV}. \quad (5)$$

With the same cutoff value, imposing the matching condition of Eq. (3) with $M_{\text{thr}} = M_{B_s} + M_K$ one finds

$$a_B(1 \text{ GeV}) = -3.41 \pm 0.02. \quad (6)$$

With this matching procedure, and considering the heavy-quark mass scaling of the low-energy constants (LECs) [9, 27]:

$$\{h_i^B\} \sim \{h_i^D\} \frac{m_B}{m_D}, \quad (7)$$

for $h_i \in \{h_{24}, h_{35}, h'_4, h'_5\}$ (for their definitions, we refer to Ref. [25]), the B_{s0}^* and B_{s1} masses can be obtained in line with HQFS [9, 10] as listed in Table 1.

With the masses and the effective couplings, which are computed from the residues of the coupled-channel T -matrix, we can update the results in Ref. [1] of the partial decay widths of the D_{s0}^* and D_{s1} mesons by recalculating the Feynman diagrams therein in the hadronic molecular picture using the updated values of the involved meson masses and branching fractions² and correct the results for the B_{s0}^* and B_{s1} .

²In particular, the D^{*+} width is much more precisely known [28]. The updated parameter values are: for the axial coupling $g_\pi = 0.566 \pm 0.006$; for those related to the magnetic coupling, $1/\beta = 335$ MeV, $m_c = 1304$ MeV, and $m_b = 4660$ MeV. See Ref. [1] for the definitions of the parameters.

Table 2: Hadronic partial decay widths of D_{s0}^* , D_{s1} , B_{s0}^* and B_{s1} as hadronic molecules (in units of keV) computed with the diagrams shown in Fig. 2. The second and third columns correspond to the contributions from loops (Fig. 2 (a) and (b)), and the π^0 - η mixing (Fig. 2 (c)), respectively. Here the central values are obtained using the central values of the parameters h_i 's and $a(\mu)$ given in Table VIII in Ref. [25], and the uncertainties are propagated from those of the parameters.

Decay channel	Loops	π^0 - η mixing	Full result
$D_{s0}^* \rightarrow D_s \pi^0$	50 ± 3	20 ± 2	132 ± 7
$D_{s1} \rightarrow D_s^* \pi^0$	37 ± 7	20 ± 3	111 ± 15
$B_{s0}^* \rightarrow B_s \pi^0$	15 ± 2	22 ± 3	75 ± 6
$B_{s1} \rightarrow B_s^* \pi^0$	16 ± 2	23 ± 3	76 ± 7

The results for the isospin breaking hadronic partial decay widths are shown in Table 2,³ and those for the radiative partial decay widths are given in Table 3. Mainly because of the change of phase spaces, the results for the bottom mesons presented here, except for the $B_{s1} \rightarrow B_{s0}^* \gamma$ transition, are much larger than those in Ref. [1] that used too small B_{s0}^* and B_{s1} masses, and supersede the results therein. In Fig. 1, we show the dependence of the hadronic decay widths of the B_{s0}^* and B_{s1} on the mass differences $\Delta_{B_s} = M_{B_{s0}^*} - M_{B_s}$ and $\Delta_{B_s^*} = M_{B_{s1}} - M_{B_s^*}$, respectively. One clearly sees the quick increase of the results as the mass differences get larger. From comparing the hadronic and radiative decay widths, one sees that the preferred decay modes for the B_{s0}^* and B_{s1} are $B_s \pi^0$, the $B_s \gamma$, respectively.

For the calculation of the hadronic decay widths, the formulation is almost exactly the same as that in Ref. [1] and is not repeated here (see Ref. [1] for details). There is, however, one crucial difference.

In Ref. [1], the hadronic decay widths are split into two kinds of contributions, namely that from the π^0 - η mixing, and that from DK loops due to the mass differences between the charged and neutral D and K mesons. They are shown in Fig. 2 (c) and (a), respectively. The hadronic width obtained in that way for the $D_{s0}^*(2317)$ is (95 ± 5) keV [1].⁴ The width may also be related to twice the imaginary part of the pole in the complex energy plane. For comparison, in Table 4 we also give the poles obtained by considering isospin breaking in the T -matrix in the particle basis (the

³Since the widths are sensitive the masses of the involved particles, in order to get the proper hadronic decay width of the $D_{s1}(2460)$, the matching procedure described above should also be done at the D^*K threshold to determine the value of $a(\mu)$ in this case. And the scaling in Eq. (7) with m_B replaced by m_{D^*} is also necessary. Otherwise, the width of the $D_{s1}(2460)$ would be much smaller.

⁴The error quoted here is smaller than that in Ref. [1] as there was a typo in the code for the π^0 - η mixing used therein.

Table 3: Radiative partial decay widths of D_{s0}^* , D_{s1} , B_{s0}^* and B_{s1} as hadronic molecules (in units of keV). Here EC, MM and CT represent the contributions from only the electric coupling, the magnetic moment, and the contact term, respectively; “-” means that there is no such contribution; “?” means that the corresponding contact term is unknown and the full result cannot be obtained without additional input. See Ref. [1] for details. Remark that we have recalculated the value of coupling of the contact term (κ in Ref. [1]) and now its value is too small compared with the uncertainty. Therefore we did not list the uncertainty from the contact term contribution.

Decay channel	EC	MM	CT	Full result
$D_{s0}^* \rightarrow D_s^* \gamma$	3.5 ± 0.3	0.06 ± 0.02	0.04	3.7 ± 0.3
$D_{s1} \rightarrow D_s \gamma$	13 ± 1	6.5 ± 0.6	0.1	42 ± 4
$D_{s1} \rightarrow D_s^* \gamma$	12 ± 2	0.8 ± 0.1	0.1	13 ± 2
$D_{s1} \rightarrow D_{s0}^* \gamma$	-	3.0 ± 0.6	?	?
$B_{s0}^* \rightarrow B_s^* \gamma$	58 ± 8	2.1 ± 0.3	0.02	59 ± 8
$B_{s1} \rightarrow B_s \gamma$	70 ± 10	41 ± 6	0.02	220 ± 31
$B_{s1} \rightarrow B_s^* \gamma$	110 ± 15	0.20 ± 0.02	0.03	100 ± 15
$B_{s1} \rightarrow B_{s0}^* \gamma$	-	0.03 ± 0.01	?	?

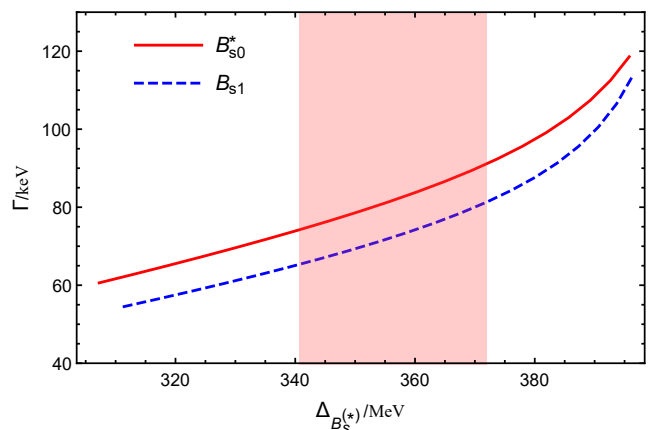


Fig. 1: Dependence of the hadronic decay widths of the B_{s0}^* and B_{s1} on the mass differences $\Delta_{B_s} = M_{B_{s0}^*} - M_{B_s}$ and $\Delta_{B_s^*} = M_{B_{s1}} - M_{B_s^*}$, for the subtraction constant $a_B(1 \text{ GeV})$ in the region from -3.31 to -3.51 , covering the range in Eq. (6) (shaded in the plot).

channels are $D^+ K^0, D^0 K^+, D_s^+ \eta$ and $D_s^+ \pi^0$) using the same LECs. One sees that the result for the $D_{s0}^*(2317)$ in Ref. [1] is smaller than that in Table 4; the same also happens for the $D_{s1}(2460)$.

We find that the main reason for the difference is that in the transition vertex $D^+ K^0 (D^0 K^+) \rightarrow D_s \pi^0$ denoted by the solid circle in (a), there is also a subleading isospin breaking contribution, which was, however, neglected in Ref. [1].

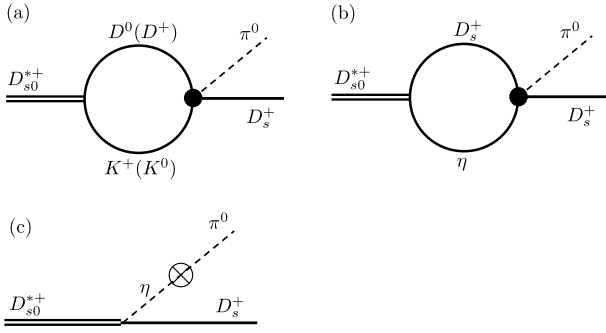


Fig. 2: The diagrams for the hadronic decay mode $D_{s0}^* \rightarrow D_s^+ \pi^0$. (a), with isospin conserving $D^{+(0)} K^{0(+)} \rightarrow D_s^+ \pi^0$ four-point vertices, and (c) were considered in Ref. [1]. Here we consider all these three diagrams and four-point vertices with isospin breaking effects.

Table 4: Masses and hadronic partial decay widths of D_{s0}^* , D_{s1} , B_{s0}^* and B_{s1} computed from searching for poles in the complex energy plane of the T -matrices in the particle basis. The mass and width correspond to the real part and twice the absolute values of the imaginary part of the pole location, respectively.

Meson	Mass [MeV]	Hadronic width (pole) [keV]
D_{s0}^*	2318 (fixed)	120_{-4}^{+18}
D_{s1}	2458_{-17}^{+15}	102_{-11}^{+27}
B_{s0}^*	5722 ± 14	75_{-9}^{+24}
B_{s1}	5774 ± 13	74_{-8}^{+23}

Here, we keep these isospin breaking terms in the four-point transition vertices ($D^+ K^0(D^0 K^+) \rightarrow D_s \pi^0$ and analogous transitions for other heavy-strange sectors) as derived from the next-to-leading order chiral Lagrangian [20], and consider further Fig. 2 (b) for self-consistency.⁵ It is found that the contributions from loops increase sizeably compared with those given in Ref. [1], and consequently the hadronic widths obtained in this way, see Table 2, almost recover those from pole searching (Table 4).

The results are consistent with all the available experimental information. In Table 5, we show a comparison for the following ratios of partial widths to the available data

⁵It turns out that the contribution from Fig. 2 (b) is negligible since the amplitude is proportional to the low-energy constant h_0 , which is much smaller than the other h_i 's [25].

Table 5: Comparison of the updated results for the ratios of partial widths defined in Eq. (8) with the experimental data. The central value of R_2 is fixed to reproduce the central measured value to determine the parameter for contact term in radiative decays (for details, see Ref. [1]).

Ratio	Our Result	Measured value
R_1	0.028 ± 0.009	< 0.059
R_2	$0.38(\text{fixed}) \pm 0.08$	0.38 ± 0.05
R_3	0.12 ± 0.02	< 0.16
R_4	0.028 ± 0.006	< 0.22
R_5	0.97 ± 0.01	0.93 ± 0.09
R_6	0.37 ± 0.08	0.35 ± 0.04
R_7	0.12 ± 0.02	< 0.24
R_8	0.027 ± 0.004	< 0.25

and an update of the corresponding results in Ref. [1]:

$$\begin{aligned}
 R_1 &= \frac{\Gamma(D_{s0}^* \rightarrow D_s^* \gamma)}{\Gamma(D_{s0}^* \rightarrow D_s \pi^0)}, & R_2 &= \frac{\Gamma(D_{s1} \rightarrow D_s \gamma)}{\Gamma(D_{s1} \rightarrow D_s^* \pi^0)}, \\
 R_3 &= \frac{\Gamma(D_{s1} \rightarrow D_s^* \gamma)}{\Gamma(D_{s1} \rightarrow D_s^* \pi^0)}, & R_4 &= \frac{\Gamma(D_{s1} \rightarrow D_{s0}^* \gamma)}{\Gamma(D_{s1} \rightarrow D_s^* \pi^0)}, \\
 R_5 &= \frac{\Gamma(D_{s1} \rightarrow D_s^* \pi^0)}{\Gamma(D_{s1} \rightarrow D_s^* \pi^0) + \Gamma(D_{s1} \rightarrow D_{s0}^* \gamma)}, \\
 R_6 &= \frac{\Gamma(D_{s1} \rightarrow D_s \gamma)}{\Gamma(D_{s1} \rightarrow D_s^* \pi^0) + \Gamma(D_{s1} \rightarrow D_{s0}^* \gamma)}, \\
 R_7 &= \frac{\Gamma(D_{s1} \rightarrow D_s^* \gamma)}{\Gamma(D_{s1} \rightarrow D_s^* \pi^0) + \Gamma(D_{s1} \rightarrow D_{s0}^* \gamma)}, \\
 R_8 &= \frac{\Gamma(D_{s1} \rightarrow D_{s0}^* \gamma)}{\Gamma(D_{s1} \rightarrow D_s^* \pi^0) + \Gamma(D_{s1} \rightarrow D_{s0}^* \gamma)}.
 \end{aligned} \tag{8}$$

Our results are also consistent with the the branching fraction of the $D_{s0}^* \rightarrow D_s \pi^0$, ($1.00_{-0.20}^{+0.00}$), measured recently by the BESIII Collaboration [29].

To summarize, we update the results reported in Ref. [1] for the widths of the lightest scalar heavy light mesons in the molecular approach, since some input parameters are now known with a higher accuracy, part of the isospin breaking sources was missing in Ref. [1] and, most importantly, the bottom-strange meson masses used therein were too small by about 100 MeV compared to expectations deduced from HQFS. We traced this discrepancy to some HQFS violation in the regularization procedure for the two meson loops coded in Ref. [1]. The results presented here should be useful for the search of the lowest positive-parity bottom-strange mesons, with the $B_s \pi^0$ and $B_s \gamma$ being the preferred searching channels for B_{s0}^* and B_{s1} , respectively, and revealing the internal structure of the charmed ones.

Acknowledgments

This work is supported in part by the National Natural Science Foundation of China (NSFC) and the Deutsche Forschungsgemeinschaft (DFG, German Research Foundation) through the funds provided to the Sino-German Collaborative Research Center “Symmetries and the Emergence of Structure in QCD” (NSFC Grant No. 12070131001, DFG Project-ID 196253076 – TRR110), by NSFC under Grants No. 11835015, No. 12047503 and No. 11961141012, by the Chinese Academy of Sciences (CAS) under Grants No. XDPB15, No. XDB34030000 and No. QYZDB-SSW-SYS013, by CAS through a President’s International Fellowship Initiative (PIFI) (Grant No. 2018DM0034), by the VolkswagenStiftung (Grant No. 93562), by the EU Horizon 2020 research and innovation programme, STRONG-2020 project under grant agreement No 824093, and by the US Department of Energy under contract DE-SC0015393.

References

1. M. Cleven, H. W. Griebhammer, F.-K. Guo, C. Hanhart and U.-G. Meißner, *Eur. Phys. J. A* **50** (2014) 149 [[arXiv:1405.2242](#) [hep-ph]].
2. B. Aubert *et al.* [BaBar], *Phys. Rev. Lett.* **90** (2003) 242001 [[arXiv:hep-ex/0304021](#) [hep-ex]].
3. D. Besson *et al.* [CLEO], *Phys. Rev. D* **68** (2003) 032002 [erratum: *Phys. Rev. D* **75** (2007) 119908] [[arXiv:hep-ex/0305100](#) [hep-ex]].
4. F.-K. Guo, C. Hanhart, U.-G. Meißner, Q. Wang, Q. Zhao and B.-S. Zou, *Rev. Mod. Phys.* **90** (2018) 015004 [[arXiv:1705.00141](#) [hep-ph]].
5. M. A. Nowak, M. Rho and I. Zahed, *Acta Phys. Polon. B* **35** (2004) 2377 [[arXiv:hep-ph/0307102](#) [hep-ph]].
6. W. A. Bardeen, E. J. Eichten and C. T. Hill, *Phys. Rev. D* **68** (2003) 054024 [[arXiv:hep-ph/0305049](#) [hep-ph]].
7. N. N. Achasov, S. A. Devyanin and G. N. Shestakov, *Phys. Lett. B* **88** (1979) 367.
8. C. Hanhart, B. Kubis and J. R. Pelaez, *Phys. Rev. D* **76** (2007) 074028 [[arXiv:0707.0262](#) [hep-ph]].
9. M. Albaladejo, P. Fernandez-Soler, F.-K. Guo and J. Nieves, *Phys. Lett. B* **767** (2017) 465 [[arXiv:1610.06727](#) [hep-ph]].
10. M.-L. Du, M. Albaladejo, P. Fernández-Soler, F.-K. Guo, C. Hanhart, U.-G. Meißner, J. Nieves and D. L. Yao, *Phys. Rev. D* **98** (2018) 094018 [[arXiv:1712.07957](#) [hep-ph]].
11. F.-K. Guo, P.-N. Shen, H.-C. Chiang, R. G. Ping and B. S. Zou, *Phys. Lett. B* **641** (2006) 278 [[arXiv:hep-ph/0603072](#) [hep-ph]].
12. F.-K. Guo, P.-N. Shen and H.-C. Chiang, *Phys. Lett. B* **647** (2007) 133 [[arXiv:hep-ph/0610008](#) [hep-ph]].
13. E. E. Kolomeitsev and M. F. M. Lutz, *Phys. Lett. B* **582** (2004) 39 [[arXiv:hep-ph/0307133](#) [hep-ph]].
14. C. B. Lang, D. Mohler, S. Prelovsek and R. M. Woloshyn, *Phys. Lett. B* **750** (2015) 17 [[arXiv:1501.01646](#) [hep-lat]].
15. A. Faessler, T. Gutsche, V. E. Lyubovitskij and Y. L. Ma, *Phys. Rev. D* **76** (2007) 014005 [[arXiv:0705.0254](#) [hep-ph]].
16. D. Gamermann, L. R. Dai and E. Oset, *Phys. Rev. C* **76** (2007) 055205 [[arXiv:0709.2339](#) [hep-ph]].
17. A. Faessler, T. Gutsche, V. E. Lyubovitskij and Y. L. Ma, *Phys. Rev. D* **76** (2007) 114008 [[arXiv:0709.3946](#) [hep-ph]].
18. M. F. M. Lutz and M. Soyeur, *Nucl. Phys. A* **813** (2008) 14 [[arXiv:0710.1545](#) [hep-ph]].
19. A. Faessler, T. Gutsche, V. E. Lyubovitskij and Y.-L. Ma, *Phys. Rev. D* **77** (2008) 114013 [[arXiv:0801.2232](#) [hep-ph]].
20. F.-K. Guo, C. Hanhart, S. Krewald and U.-G. Meißner, *Phys. Lett. B* **666** (2008) 251 [[arXiv:0806.3374](#) [hep-ph]].
21. C.-J. Xiao, D. Y. Chen and Y.-L. Ma, *Phys. Rev. D* **93** (2016) 094011 [[arXiv:1601.06399](#) [hep-ph]].
22. X.-Y. Guo, Y. Heo and M. F. M. Lutz, *Phys. Rev. D* **98** (2018) 014510 [[arXiv:1801.10122](#) [hep-lat]].
23. S. Fajfer and A. Prapotnik Brdnik, *Phys. Rev. D* **92** (2015) 074047 [[arXiv:1506.02716](#) [hep-ph]].
24. S. Fajfer and A. Prapotnik Brdnik, *Eur. Phys. J. C* **76** (2016) 537 [[arXiv:1606.06943](#) [hep-ph]].
25. L. Liu, K. Orginos, F.-K. Guo, C. Hanhart and U.-G. Meißner, *Phys. Rev. D* **87** (2013) 014508 [[arXiv:1208.4535](#) [hep-lat]].
26. J. A. Oller and U.-G. Meißner, *Phys. Lett. B* **500** (2001) 263 [[arXiv:hep-ph/0011146](#) [hep-ph]].
27. M. Cleven, F.-K. Guo, C. Hanhart and U.-G. Meißner, *Eur. Phys. J. A* **47** (2011) 19 [[arXiv:1009.3804](#) [hep-ph]].
28. P. A. Zyla *et al.* [Particle Data Group], *PTEP* **2020** (2020) 083C01 and the 2021 update.
29. M. Ablikim *et al.* [BESIII], *Phys. Rev. D* **97** (2018) 051103 [[arXiv:1711.08293](#) [hep-ex]].